# Chain-Stiffness and Lyotropic Liquid Crystallinity of Polysilylene Bearing (*S*)-2-Methylbutyl and *n*-Decyl Substituents

**Tomoko Natsume, Libin Wu, and Takahiro Sato***

*Department of Macromolecular Science, Osaka University and CREST of Japan Science and Technology, 1-1 Machikaneyama-cho, Toyonaka, Osaka 560-0043, Japan*

**Ken Terao and Akio Teramoto**

*Research Organization of Science and Engineering, Ritsumeikan University and CREST of Japan Science and Technology, Nojihigashi 1-1-1, Kusatsu, Siga 525-8577, Japan*

**Michiya Fujiki**

*NTT Basic Research Laboratories, NTT Corporation and CREST of Japan Science and Technology, 3-1 Wakamiya, Morinosato, Atsugi, Kanagawa 243-0198, Japan*

*Received June 18, 2001; Revised Manuscript Received August 13, 2001*

ABSTRACT: The intrinsic viscosity [$\eta$], the radius of gyration $\langle S^2\rangle^{1/2}$, and the isotropic−cholesteric phase boundary concentration $c_I$ (between the isotropic and biphasic regions) for poly[(*n*-decyl-(*S*)-2-methylbutyl)-silylene] dissolved in isooctane were measured as functions of the weight-average molecular weight $M_w$. By analyzing the results of [$\eta$] and $\langle S^2\rangle^{1/2}$ in terms of the wormlike-chain model, the persistence length $q$ was determined to be 70 nm. Using this $q$, the scaled particle theory for the hard wormlike-spherocylinder model successfully predicted $c_I$ at high $M_w$ but underestimated it at low $M_w$. The underestimate may be ascribed to the flexibility effect in the vicinity of the polymer-chain ends on $c_I$, which is more appreciable than the same effect on [$\eta$].

## Introduction

Recently, it has been found that the silicon backbone of some alkyl-substituted polysilylenes take a rigid helical conformation in solution[1−3] due to severe restriction of their internal rotation by steric hindrance between neighboring alkyl side chains. For example, the persistence length of poly[(*n*-hexyl-(*S*)-2-methylbutyl)-silylene] (PH2MBS) is reported to be 85 nm,[2] indicating that this polysilylene is even stiffer than typical stiff polymers, e.g., poly(hexyl isocyanate) (20−43 nm), aromatic polyamides (20−50 nm), and the double helix of DNA (ca. 60 nm).[4]

It is well-known that the polymer chain stiffness closely correlates to liquid crystallinity.[4] Thus, we have examined lyotropic liquid crystallinity of an isooctane solution of PH2MBS with increasing the polymer concentration. Unfortunately, due to the limiting solubility of PH2MBS, we could not observe any liquid crystal phase but observed a gel in its concentrated isooctane solution. To enhance solubility, we replaced the hexyl side chain of PH2MBS by an *n*-decyl chain and found a cholesteric phase in concentrated isooctane solutions of poly((*n*-decyl-(*S*)-2-methylbutyl)silylene) (PD2MBS; cf. Scheme 1). Very recently, Watanabe, Kamee, and Fujiki[5] found liquid crystallinity also in the bulk phase of PD2MBS with relatively low molecular weights. Therefore, this polysilylene is a unique polymer, exhibiting both lyotropic and thermotropic liquid crystallinity.

This paper reports the persistence length and the isotropic−cholesteric phase boundary concentration of PD2MBS in isooctane solutions. The resulting persistence length and phase boundary concentration are compared with each other through a standard statistical−mechanical theory, the scaled particle theory for stiff polymer solutions.[4]

**Scheme 1**

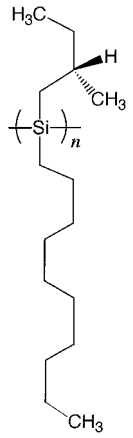


## Experimental Section

**Polymer Samples.** Dichlorosilane monomer bearing (*S*)-2-methylbutyl and *n*-decyl substituents was polymerized in hot toluene by the Wurtz-type condensation.[6] The polymer sample obtained was recovered from the toluene solution, and divided into many fractions by repeating fractional precipitation, using cyclohexane as the solvent and ethanol as the precipitant. The fractionation was made in brownish glassware to avoid photodegradation of the sample. Ten middle fractions were chosen for the following experiments. The polydispersity in the molecular weight of the fractions were checked by size-exclusion chromatography (SEC) with a column of Shodex KF-806 M and using 40 °C tetrahydrofuran as the eluent. Ratios of the weight- to number-average molecular weight $M_w/M_n$ estimated by SEC were 1.04−1.14 (except for one sample used for the isotropic−cholesteric phase boundary concentration);[7] the calibration curve was made using eight PD2MBS samples whose weight-average molecular weights $M_w$ were determined by light scattering and/or sedimentation equilibrium (see below).

10.1021/ma0110352 CCC: $20.00 
Published on Web 09/29/2001

**Light Scattering.** Light scattering measurements for isooctane solutions of five PD2MBS samples were made at 25 °C on a DAWN DSP multiangle light scattering instrument (Wyatt Technology Inc.) equipped with a flow cell, to determine $M_w$, the second virial coefficient $A_2$, and $z$-average radius of gyration $\langle S^2\rangle_z^{1/2}$. The light source was a He−Ne laser emitting 633 nm vertically polarized light. The detailed procedure for the measurements is described in ref 6.

Specific refractive index increments $\partial n/\partial c$ of PD2MBS in 25 °C isooctane were measured to be 0.180 cm$^3$/g at 436 nm and 0.161 cm$^3$/g at 546 nm, using a modified Schulz−Cantow type differential refractometer. The value of $\partial n/\partial c$ at 633 nm was obtained to be 0.153 cm$^3$/g by extrapolation of the results at 436 and 546 nm, using the Couchy dispersion formula.

**Sedimentation Equilibrium.** For four lower molecular weight PD2MBS samples, $M_w$ and $A_2$ were determined in isooctane at 25 °C by sedimentation equilibrium using a Beckman Optima XL-I analytical ultracentrifuge equipped with the Rayleigh interferometer with a 675 nm diode laser as light source. Test solutions and solvent were put in aluminum 12 mm double sector cells, and rotated at 8000−18 000 rpm. Data analysis is explained in ref 6.

The partial specific volume and $\partial n/\partial c$ at 675 nm of PD2MBS in 25 °C isooctane are necessary to the data analysis. The former was determined to be 1.107 cm$^3$/g using an Anton Paar DMA 5000 oscillation U-tube densitometer, while the latter was estimated to be 0.149 cm$^3$/g by extrapolation of the results at 436 and 546 nm (see above).

**Viscometry.** Viscosities of isooctane solutions of eight PD2MBS samples were measured by a conventional Ubbelohde-type capillary viscometer to determine the intrinsic viscosity $[\eta]$. For the two highest molecular weight PD2MBS samples, solution viscosities were also measured with a four-bulb low-shear viscometer, and weak shear-rate dependencies were found. Thus, $[\eta]$ for the two samples were obtained by extrapolation to the zero-shear rate.

**Determination of Isotropic-Liquid Crystal Phase Boundary Concentration.** When the concentration of an isooctane solution of a PD2MBS sample was increased, the solution exhibited strong optical birefringence above some critical concentration, under a polarizing microscope. This birefringence indicates the formation of a liquid crystal phase in the isooctane solution of PD2MBS. The critical mass concentration $c_I$ of the appearance or disappearance of the birefringence was determined for isooctane solutions of six PD2MBS samples, with increasing or decreasing the polymer concentration. This concentration corresponds to the phase boundary concentration between the isotropic and biphasic regions. Owing to the limiting amounts of PD2MBS samples used, it was difficult to analyze coexisting isotropic and liquid-crystal phases separately, so that another phase boundary concentration between the biphasic and liquid-crystal region was not determined in this study.

## Results and Discussion

**Intrinsic Viscosity and Radius of Gyration.** Figure 1 shows the molecular weight dependence of the intrinsic viscosity $[\eta]$ of PD2MBS in isooctane at 25 °C (circles). In the double-logarithmic plot, the data points obey a curve convex upward, whose slope is 1.5 at $M_w < 2 \times 10^5$. This strong molecular weight dependence indicates the chain stiffness of PD2MBS. The stiffness of the PD2MBS chain is also indicated by data of the radius of gyration $\langle S^2\rangle_z^{1/2}$, which is almost proportional to $M_w^{0.8}$ as shown in Figure 2.

The data of $[\eta]$ and $\langle S^2\rangle_z^{1/2}$ shown in Figures 1 and 2, respectively, are analyzed in terms of the wormlike-chain model to determine the chain stiffness parameter, the persistence length $q$.[8] Recently, the same analysis was made for poly(*n*-hexyl-(*S*)-2-methylbutyl)silylene) (PH2MBS) and poly(*n*-hexyl-(*S*)-3-methylpentyl)silylene) (PH3MPS) in the same solvent,[2] and it turned out that

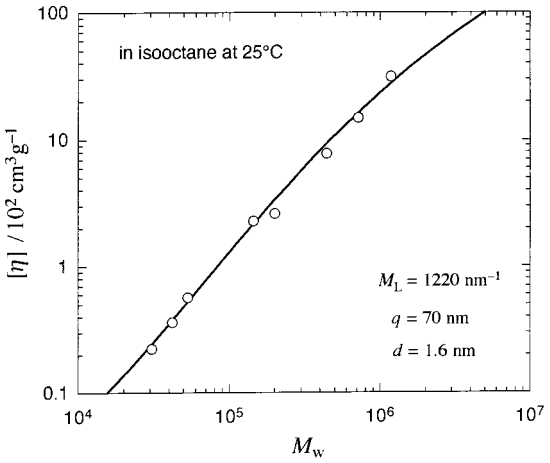


**Figure 1.** Molecular weight dependence of the intrinsic viscosity of PD2MBS in isooctane at 25 °C: circles, experimental data; solid curve, theoretical values calculated by the Yamakawa−Fujii−Yoshizaki theory[11,12] for the wormlike-cylinder model with the parameters indicated.

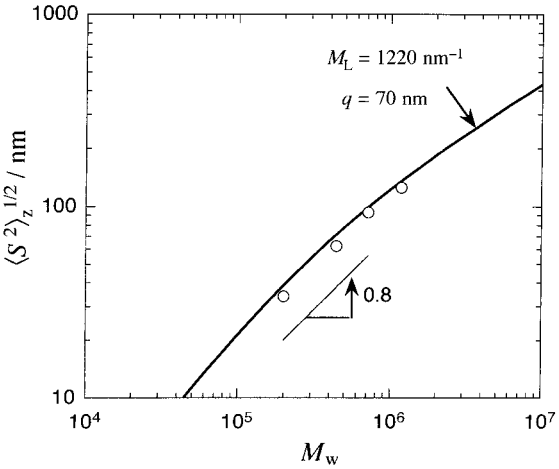


**Figure 2.** Molecular weight dependence of the radius of gyration of PD2MBS in isooctane at 25 °C: circles, experimental data; solid curve, theoretical values calculated by the Benoit−Doty theory[13] for the wormlike-chain model with the parameters indicated.

local conformations of PH2MBS and PH3MPS are almost identical with that of the $^7/_3$ helix proposed for poly((di-*n*-pentyl)silylene) and poly((di-*n*-butyl)silylene) in crystalline state.[9,10] From the resemblance of the chemical structure between PD2MBS and PH2MBS, we may expect that the local conformation of PD2MBS is also approximated to the $^7/_3$ helical conformation. Using the helix pitch per the monomer unit to be 0.197 nm,[9] the molar mass per unit contour length $M_L$ for PD2MBS is estimated to be 1220 nm$^{-1}$.

According to the theory of Yamakawa, Fujii, and Yoshizaki[11,12] for the wormlike-cylinder model, $[\eta]$ can be calculated as a function of the molecular weight, if $M_L$, $q$, and the cylinder diameter $d$ are given. A trial-and-error method was used to find $q$ and $d$ values which lead to the closest agreement between the Yamakawa−Fujii−Yoshizaki theory and experimental $[\eta]$ with $M_L$ fixed to 1220 nm$^{-1}$. It is shown by the solid curve in Figure 1 that when $q$ and $d$ are chosen to be 70 nm and 1.6 nm, respectively, the theory fits closely the data points. Since $d$ affects $[\eta]$ only at low molecular weights, the value of $q$ was almost uniquely determined irrespective of the $d$ value.

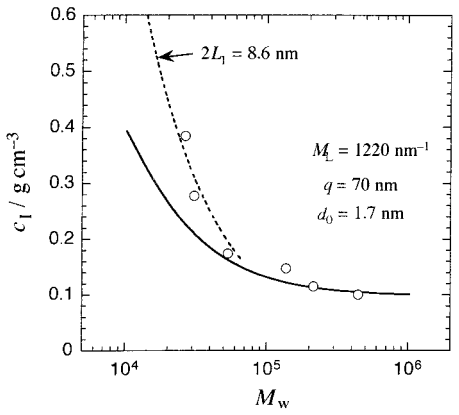


**Figure 3.** Molecular weight dependence of the isotropic−cholesteric phase boundary concentration $c_I$ between the isotropic and biphasic regions of isooctane solutions of PD2MBS: circles, experimental data; solid curve, theoretical values calculated by the scaled particle theory (SPT) for the hard wormlike-spherocylinder model[4] with the parameters indicated; dashed curve: theoretical values calculated by the SPT for the hard-tailed-wormlike-spherocylinder model with $2L_1 = 8.6$ nm (cf. Figure 4a).

The solid curve in Figure 2 shows theoretical values of $\langle S^2\rangle^{1/2}$ calculated by the Benoit−Doty equation[13] for the wormlike chain with $M_L = 1220$ nm$^{-1}$ and $q = 70$ nm. The curve almost fits the data points, though a better fit is obtained by using a slightly larger $M_L$.

The $q$ value of PD2MBS is close to that of PH2MBS (=85 nm) and much longer than that of PH3MPS (=6.2 nm), confirming the previous conclusion[2] that a polysilylene with a $\beta$-branched alkyl side-chain is much stiffer compared to those without it. The persistence length of helical polymers is determined by the steepness of the internal-rotation potential in the main chain.[14] The slightly shorter $q$ of PD2MBS than that of PH2MBS implies that the longer nonbranched alkyl side-chain makes the internal-rotation potential of the silicon backbone less steep.

**Isotropic—Liquid Crystal Phase Boundary Concentration.** Figure 3 shows the molecular weight dependence of the isotropic−liquid crystal (cholesteric) phase boundary concentration $c_I$ for isooctane solutions of PD2MBS by circles. It is almost molecular-weight independent in the high $M_w$ region, but sharply increases with decreasing $M_w$. Recently, Watanabe, Kamee, and Fujiki[5] found a cholesteric phase in PD2MBS in the bulk at $M_w \gtrsim 1.8 \times 10^4$. The strong $M_w$ dependence of our lyotropic $c_I$ data at low $M_w$ is not inconsistent with their critical molecular weight for the thermotropic liquid crystallinity; the specific volume (corresponding to $c_I$) of the bulk PD2MBS is about 0.98 cm$^3$/g.

It is known that the isotropic−liquid crystal phase boundary concentration of stiff−polymer solutions is quantitatively predicted by the scaled particle theory (SPT) for hard wormlike spherocylinders,[4] which is a standard statistical−mechanical theory for stiff polymer solutions, being briefly explained in Appendix A. The theory needs three molecular parameters, $M_L$, $q$, and the hard-core diameter $d_0$ of the cylinder, to calculate $c_I$. The former two parameters have already been determined from $[\eta]$ data in the previous subsection. The last parameter $d_0$ may be estimated from the partial specific volume $\bar{v}$ by the equation

$$d_0 = \left(\frac{4\bar{v}M_L}{\pi N_A}\right)^{1/2} \quad (1)$$

where $N_A$ is the Avogadro constant. Using $\bar{v} = 1.107$ cm$^3$/g (cf. Experimental Section) as well as $M_L = 1220$ nm$^{-1}$, we have a value of 1.7 nm for $d_0$ of PD2MBS.

The solid curve in Figure 3 indicates theoretical values of $c_I$ calculated by the SPT with $M_L = 1220$ nm$^{-1}$, $q = 70$ nm, and $d_0 = 1.7$ nm. The theory agrees with experimental results at high $M_w$, but underestimates $c_I$ at $M_w < 5 \times 10^4$. Especially, for the lowest molecular weight sample, the theoretical $c_I$ is almost half of the experimental one.

For other rigid helical polymers, say schizophyllan, xanthan, and poly($\gamma$-benzyl-L-glutamate), the SPT successfully predicts $c_I$ even in low molecular weight regions,[4] so that the deviation of the theoretical curve in Figure 3 may not come from invalidity of the theory itself for short chains. The Kuhn segment number of the lowest molecular weight sample in Figure 3 is as small as 0.15, and the theoretical value of $c_I$ indicated by the solid curve is almost identical with that calculated by the SPT for straight spherocylinders at such a low molecular weight. The remarkable deviation at the lowest molecular weight indicates that some residual conformational entropy remains in the short polysilylene chain in the isotropic phase.

A similar disagreement between the theory and experiment of $c_I$ was observed for solutions of polymacromonomers consisting of polystyrene with the degree of polymerization of the side chain fixed to 33.[23] The chain stiffness of both PD2MBS and polymacromonomer may come from the steric hindrance among neighboring side chains,[10] because for example poly[(di-*n*-hexyl)-silylene][15] and polystyrene are known as flexible polymers. In the middle of the main chain, each side-chain strongly interacts with neighboring side chains on the both sides along the main chain, while at the chain end, side chains may interact each other more loosely, so that the internal rotation in the backbone chain should occur more freely in the vicinity of both chain ends than in the middle of the main chain.[16] In other words, the PD2MBS and polymacromonomer chains may be more flexible in the vicinity of the chain ends than in the middle. At sufficiently high molecular weights, this flexibility effect at the chain ends may be neglected, but it becomes important with decreasing molecular weight.

## Concluding Remarks

In the above discussion, we have insisted that the disagreement between theory and experiment of the isotropic−liquid crystal phase boundary concentration $c_I$ for PD2MBS solutions comes from the flexibility effect in the vicinity of both chain ends. This insistence, however, seems to be inconsistent of the good agreement of intrinsic viscosity $[\eta]$ data with the theory for the uniform wormlike-chain model even in a low molecular weight region, shown in Figure 1. To clarify this point, we examine theoretically how strongly the flexibility at polymer end portions affects $c_I$ and $[\eta]$, respectively.

Although a wormlike-chain model with the persistence length varying along the chain contour may be suitable to discuss the present problem, it is not easy to calculate $[\eta]$ or the conformational entropy loss at the formation of the liquid crystal phase for such a model. Here we use a cruder model as a first approximation, i.e., a wormlike chain connected to freely jointed chains

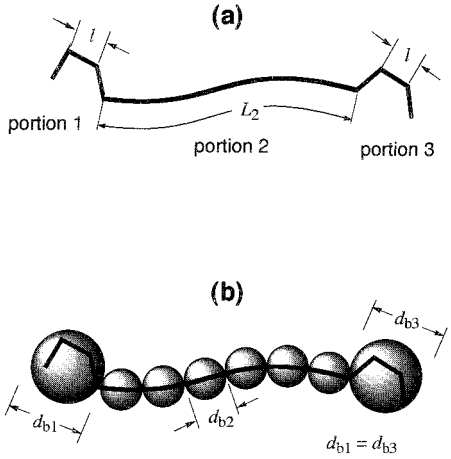


**Figure 4.** (a) Tailed-wormlike chain model. (b) Touched-bead model whose contour obeys the tailed-wormlike chain.

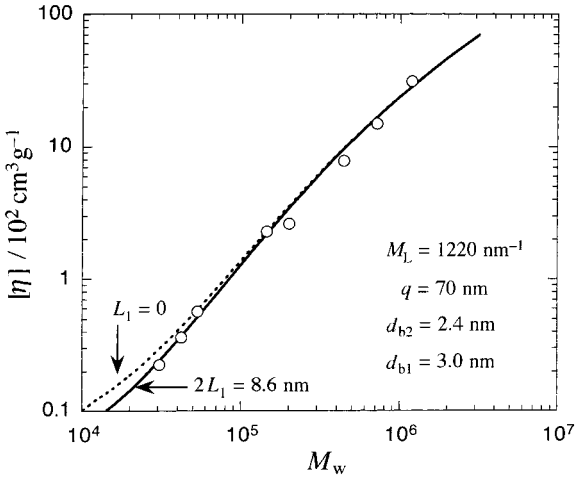


**Figure 5.** Comparison of experimental intrinsic viscosities with the theory calculated by the modified Yoshizaki−Nitta−Yamakawa theory[19] for the touched-bead model illustrated in Figure 4b.

at both ends, as schematically shown in Figure 4a (called as *the tailed-wormlike chain*). The contour lengths of the wormlike chain portion 2 and the freely jointed chain portions 1 and 3 are denoted as $L_2$, $L_1$, and $L_3$, respectively. Chain flexibilities of the portion 2 and portion 1 (or 3) are characterized in terms of the persistence length $q$ and the rodlike segment length $l$, respectively.

Using the SPT, the excess free energy for a solution of hard spherocylinders whose contour is the tailed-wormlike chain is given by eq A1 along with eqs A6−A10 in Appendix A, and the phase boundary concentration $c_I$ can be calculated from this free energy. The calculation needs the following parameters: $L_2$, $L_1 + L_3$, $q$, $l$, and $d_0$ (the hard-core diameter of the spherocylinder). Terao et al.[17] pointed out that for polymers with relatively long side chains (e.g., polymacromonomers), side chains near the main-chain ends may contribute toward apparently increasing the polymer contour length. To take this contribution into account, we calculate the total contour length $L$ ($= L_1 + L_2 + L_3$) of the tailed-wormlike spherocylinder by

$$L = \frac{M}{M_L} + \frac{d_0}{3} \tag{2}$$

where $M$ and $M_L$ are the polymer molecular weight and molar mass per unit contour length (at sufficiently high molecular weights), respectively. In eq 2, we have assumed that the end hemispheres and middle cylinder of the spherocylinder have the same density.[18]

Since we have already determined $M_L$, $q$, and $d_0$ (cf. the previous section), only $L_1 + L_3$ and $l$ are unknown parameters at the calculation of $c_I$. It turned out in the numerical calculation of $c_I$ that degree of orientation of the freely jointed chain portions at the chain ends is very low within reasonable values of $l$, and resulting $c_I$ is almost independent of $l$. Therefore, the unknown parameter is substantially only $L_1 + L_3$. As shown by the dotted curve in Figure 3, low-molecular weight data of $c_I$ can be fitted by the SPT for hard tailed-wormlike spherocylinders with choosing $L_1 + L_3 = 8.6$ nm.

In the calculation of $[\eta]$, the tailed-wormlike chain is viewed as a wormlike bead model, which consists of $N_{b2}$ beads with the diameter $d_{b2}$ and one bead with the diameter $d_{b1}$ ($= d_{b3}$) at both ends, as schematically shown in Figure 4b. The $N_{b2}$ middle and two end beads correspond to the middle wormlike-chain portion 2 and the tail portions of 1 and 3 in the tailed-wormlike chain, respectively, and the number $N_{b2}$ of the middle beads is calculated by $N_{b2} = L_2/d_{b2}$, where $L_2$ is the contour length of the middle wormlike-chain portion 2. The total contour length of our beads model is equal to $N_{b2}d_{b2} + 2d_{b1}$, and its contour is regarded to be identical with a uniform wormlike chain with the persistence length $q$. (it is noted that the total contour length of the beads model is not equal to $L$ of tailed-wormlike spherocylinder mentioned above.)

Simply extending the theory of Yoshizaki, Nitta, and Yamakawa (YNY)[19] of the intrinsic viscosity $[\eta]$ for the wormlike touched-bead model consisting of identical beads, we can calculate $[\eta]$ of our bead model, which is characterized by the four parameters $L_2$, $q$, $d_{b1}$, and $d_{b2}$. The detailed method of calculation is described in Appendix B. Among the parameters, we can calculate $d_{b1}$ from $L_1 + L_3$, $l$, and $d_{b2}$ (cf. Appendix B) and choose the same values of $L_2$, $L_1 + L_3$, $q$, and $l$ as in the calculation of $c_I$. Thus, the only remaining unknown parameter is $d_{b2}$. If we choose this value to be 2.4 nm, the theory agrees with the experimental results of $[\eta]$, as shown by the solid curve in Figure 5. The agreement between theory and experiment in Figure 5 is as satisfactory as that in Figure 3 where we used the regular wormlike-cylinder model. The value of $d_{b2}$ of the bead model corresponds to a diameter $d$ of 1.8 nm of the wormlike cylinder model ($d = 0.74d_b$).[19] This $d$ is slightly larger than that used in Figure 3. If the effect of flexibility at chain ends is neglected (i.e., $L_1 + L_3 = 0$), the YNY theory for the wormlike touched-bead model consisting of identical beads with a diameter of 2.4 nm gives the dotted curve in Figure 5, which slightly deviates from the data points at low $M_w$.

In conclusion, the flexibility in the vicinity of polymer-chain ends appreciably affects the isotropic−liquid crystal phase boundary concentration in a low molecular weight region, but its effect on the intrinsic viscosity appears only as a small change of the diameter of the polymer chain. The tailed-wormlike chain model looks too crude to describe the real PD2MBS chain, and the contour length $L_1 + L_3$ (= 8.6 nm) of the polymer end portions estimated above seems too large. In this connection, we have to mention that $c_I$ for the uniform wormlike chain is considerably higher than that for the freely jointed chain with $l = 2q$, as pointed out by

Khokhlov and Semenov.[20] Their result indicates that freely jointed chain model underestimates the conformational entropy loss in the liquid crystal phase. Therefore, if replacing freely jointed chains in the tailed wormlike chain by flexible wormlike chains, we may fit the $c_I$ data to the theory with shorter $L_1 + L_3$, in Figure 3. The shorter $L_1 + L_3$, the weaker the flexibility effect at the chain ends on $[\eta]$, so that the above conclusion is unaltered. To make more quantitative discussion, we need a novel theory based on the modified wormlike chain model with the persistence length varying along the chain contour.

## Appendix A. Calculation of the Isotropic-Liquid-Crystal Phase Boundary Concentration

Using the scaled particle theory (SPT), we can formulate thermodynamic quantities for the solution of hard wormlike spherocylinders, including all the virial terms. Details of the formulation is described in ref 4, and the final result of the excess free energy $\Delta F$ of the solution over that of the solvent reads as

$$\frac{\Delta F}{nk_BT} = \frac{\mu^\circ}{k_BT} - 1 + \ln\left(\frac{c'}{1 - vc'}\right) + \frac{B}{2}\left(\frac{c'}{1 - vc'}\right) + \frac{v'(B - 2v')}{3}\left(\frac{c'}{1 - vc'}\right)^2 + \sigma \quad \text{(A1)}$$

Here, $n$, $\mu^\circ$, and $c'$ are the number, the standard chemical potential, and the number concentration of spherocylinders in the solution, respectively, $v$ and $\sigma$ are the volume and the orientational plus conformational entropy loss parameter of each spherocylinder, respectively, and $k_BT$ is the Boltzmann constant multiplied by the absolute temperature. The parameters $B$ and $v'$ in eq A1 are defined by

$$B \equiv (\pi/2)d_0(L - d_0)^2\rho + 6v, \quad v' \equiv v + (\pi/12)d_0^3 \quad \text{(A2)}$$

where $L$ and $d_0$ are the contour length and the hard-core diameter of the spherocylinder, respectively, and $\rho$ expresses the reduction of the excluded volume between two spherocylinders due to the alignment of spherocylinders in the liquid crystal (nematic) phase.

The parameter $\rho$ is represented in terms of the (average) orientational distribution function $f(\mathbf{a})$ of the tangent vector $\mathbf{a}$ to contour points along the spherocylinder axis, by

$$\rho = (4/\pi)\int\int |\sin\gamma| f(\mathbf{a}) f(\mathbf{a}')\, d\mathbf{a}\, d\mathbf{a}' \quad [\gamma \equiv \cos^{-1}(\mathbf{a}\cdot\mathbf{a}')] \quad \text{(A3)}$$

In the isotropic solution, $\rho$ is equal to unity, and if $f(\mathbf{a})$ in the nematic phase is expressed by the Onsager trial function, $\rho$ is written as the following function of the degree of orientation parameter $\alpha$ in the trial function:[21]

$$\rho = \frac{4}{\sqrt{\pi}\alpha}\left[1 - \frac{15}{16\alpha} + \frac{105}{512\alpha^2} - O(\alpha^{-3})\right] \quad \text{(A4)}$$

Using the same trial function for $f(\mathbf{a})$, another orientation-depending parameter $\sigma$ in $\Delta F$ in the nematic phase is written as[22]

$$\sigma = \ln\alpha - 1 + \pi e^{-\alpha} + (^1/_3)N(\alpha - 1) + (5/12)\ln\{\cosh[(^2/_5)N(\alpha - 1)]\} \quad \text{(A5)}$$

with the number of Kuhn's statistical segments $N$. In the isotropic phase, $\sigma$ is equal to zero.

We can easily extend the above expression of $\Delta F$ to the system containing hard spherocylinders whose axis is represented by a wormlike chain (with the contour length $L_2$) connected by two freely jointed chains (with the contour lengths $L_1$ and $L_3$) at both ends (the *tailed-wormlike chain*), as illustrated in Figure 4a. Only differences in $\Delta F$ are expression of $B$ and $\sigma$ in the nematic phase. For tailed-wormlike spherocylinder system, $B$ in the nematic phase is written as

$$B = (\pi/2)d_0(L - d_0)^2[(1 - x)^2\rho_{11} + 2x(1 - x)\rho_{12} + x^2\rho_{22}] + 6v \quad \text{(A6)}$$

where $L$ is the total contour length ($=L_1 + L_2 + L_3$), and $x$ is defined by

$$x = L_2/(L - d_0) \quad \text{(A7)}$$

The orientation-dependent parameter $\rho_{22}$ in eq A6 is given by eq A4 where $\alpha$ is replaced by the degree of the orientation parameter $\alpha_2$ for the wormlike chain portion 2. On the other hand, since the degree of orientation for the freely jointed chain portions 1 and 3 must be weak (i.e., the degree of the orientation parameter $\alpha_1$ for the freely jointed chain portion 1 or 3 must be small) even in the liquid crystal phase, we cannot use the asymptotic expansion like eq A4 for $\rho_{11}$ and $\rho_{12}$. In a very weakly oriented state, the orientational distribution function $f_1(\mathbf{a}_1)$ for the unit vector $\mathbf{a}_1$ along each segment in the freely jointed chain portions is expressed in the series of the Legendre polynomials $P_i(\mathbf{a}_1\cdot\mathbf{n})$, where $\mathbf{n}$ is the director in the liquid crystal phase, as

$$4\pi f_1(\mathbf{a}_1) = 1 + 5\left(1 - \frac{3}{\alpha_1}\coth\alpha_1 + \frac{3}{\alpha_1^2}\right)P_2(\mathbf{a}_1\cdot\mathbf{n}) + \ldots \quad \text{(A8)}$$

Using this expression, the parameters $\rho_{11}$ and $\rho_{12}$ are calculated by[21]

$$\rho_{1s} = 1 - \frac{5}{8}\left(1 - \frac{3}{\alpha_1}\coth\alpha_1 + \frac{3}{\alpha_1^2}\right)\left(1 - \frac{3}{\alpha_s}\coth\alpha_s + \frac{3}{\alpha_s^2}\right) \quad (s = 1, 2) \quad \text{(A9)}$$

(For $f_2(\mathbf{a}_2)$ of the wormlike-chain portion, higher order terms of $P_i(\mathbf{a}_1\cdot\mathbf{n})$ are important, but these terms do not contribute to $\rho_{12}$.)

The entropy loss parameter $\sigma$ for tailed-wormlike spherocylinder can be calculated by[21]

$$\sigma = \frac{5}{2}\left(\frac{L_1 + L_3}{l}\right)\left(1 - \frac{3}{\alpha_1}\coth\alpha_1 + \frac{3}{\alpha_1^2}\right)^2 + \sigma_2 \quad \text{(A10)}$$

where $l$ is the segment length of the freely jointed chain, and $\sigma_2$ is given by eq A5 where $N$ and $\alpha$ are replaced by the number $N_2$ of Kuhn's statistical segments in the wormlike chain portion 2 and $\alpha_2$, respectively; $N_2$ is calculated by the equation $N_2 = L_2/2q$, where $q$ is the persistence length of the middle wormlike-chain portion 2.

The phase boundary concentration $c_I$ between the isotropic and biphasic regions for the tailed-wormlike spherocylinder system can be obtained by numerically solving the following four simultaneous equations: (1) the equality of the osmotic pressure in the coexisting isotropic and nematic phases, (2) the equality of the solute chemical potential in the two phases, and (3) the two free energy minimization conditions with respect to the degrees of orientation $\alpha_1$ and $\alpha_2$ in the nematic phase.

## Appendix B. Calculation of the Intrinsic Viscosity for the Tailed-Wormlike Chain

Yoshizaki, Nitta, and Yamakawa (YNY)[19] calculated the intrinsic viscosity $[\eta]$ for the helical wormlike touched-bead model consisting of identical beads. Their equation of $[\eta]$ is written in the form

$$[\eta] = [\eta]_{KR} + [\eta]_E \tag{B1}$$

In the equation, $[\eta]_{KR}$ is the Kirkwood−Riseman term of $[\eta]$ for the helical wormlike chain, and in the wormlike KP chain limit, it is calculated by

$$[\eta]_{KR} = 6^{3/2}\,\Phi_0\Gamma_{KP}\frac{\langle S^2\rangle^{3/2}}{M} \tag{B2}$$

where $\Phi_0$ is the Flory−Fox constant ($=2.87 \times 10^{23}$), $\langle S^2\rangle$ and $M$ are the mean square radius of gyration and molecular weight of the wormlike chain, respectively, and $\Gamma_{KP}$ is a factor depending on the persistence length, the number of Kuhn's statistical segments, and the spacing between neighboring friction points on the wormlike chain (being equal to the bead spacing). On the other hand, $[\eta]_E$ in eq B1 is the Einstein intrinsic viscosity for a rigid sphere multiplied by the number of beads.

Extending the YNY theory, we calculate $[\eta]$ for our touched-bead model consisting of $N_{b2} + 2$ nonidentical beads, as illustrated in Figure 4b. The Kirkwood−Riseman term may be calculated using the three parameters, the persistence length $q$ of the middle portion, the Kuhn segment number calculated by $L_b/2q$ ($L_b = N_{b2}d_{b2} + 2d_{b1}$), and the spacing $\bar{d}_b$ between neighboring friction points on the wormlike chain, being calculated by

$$\bar{d}_b = \frac{N_{b2}d_{b2} + 2d_{b1}}{N_{b2} + 2} \tag{B3}$$

On the other hand, the Einstein intrinsic viscosity term $[\eta]_E$ is given by

$$[\eta]_E = \frac{5\pi N_A}{12M}(N_{b2}d_{b2}{}^3 + 2d_{b1}{}^3) \tag{B4}$$

where $N_A$ is the Avogadro constant.

We need the value of $d_{b1}$ to calculate $[\eta]$ for our touched-bead model using eqs B1−B4. This value may be determined in the following way. When $N_{b2}$ is equal to zero, eq B1 gives the intrinsic viscosity $[\eta]_{DB}$ of the dumbbell with the bead diameter $d_{b1}$. In the same limiting case, the tailed-wormlike chain becomes freely jointed chain with $(L_1 + L_3)/l$ segments ($l$: the segment length), whose intrinsic viscosity $[\eta]_{FJC}$ may be calculated by the YNY theory for the wormlike touched-bead model with the contour length $L_1 + L_3$, the persistence length $l/2$, and the bead diameter $d_{b2}$ (assumed to be the same as that of the middle bead). We choose the value $d_{b1}$, which equates $[\eta]_{DB}$ with $[\eta]_{FJC}$.

**Acknowledgment.** We are grateful to Prof. Junji Watanabe in Tokyo Institute of Technology for a valuable discussion about liquid crystallinity of PD2MBS, and also to Drs. Kei-ichi Torimitsu and Hideaki Takayanagi for generous support at NTT during the course of this study.

**Supporting Information Available:** Table 1, giving numerical results of the weight-average molecular weight, the radius of gyration, the intrinsic viscosity, and the isotropic−cholesteric phase boundary concentration for our PD2MBS samples. This material is available free of charge via the Internet at http://pubs.acs.org.

## References and Notes

(1) Fujiki, M. *J. Am. Chem. Soc.* **1996**, *118*, 7424.
(2) Terao, K.; Terao, Y.; Teramoto, A.; Nakamura, N.; Terakawa, I.; Sato, T.; Fujiki, M. *Macromolecules* **2001**, *34*, 2682.
(3) Fujiki, M. *Macromol. Rapid Commun.* **2001**, *22*, 539.
(4) Sato, T.; Teramoto, A. *Adv. Polym. Sci.* **1996**, *126*, 85.
(5) Watanabe, J.; Kamee, H.; Fujiki, M. *Polym. J.* **2001**, *33*, 495.
(6) Terao, K.; Terao, Y.; Teramoto, A.; Nakamura, N.; Fujiki, M.; Sato, T. *Macromolecules* **2001**, *34*, 4519.
(7) One sample ($M_w = 13.7 \times 10^4$) used for the phase boundary concentration measurement has a slightly broad molecular weight distribution with $M_w/M_n = 1.31$.
(8) Yamakawa, H. *Helical Wormlike Chains in Polymer Solutions*; Springer-Verlag: Berlin, and Heidelberg, Germany, 1997.
(9) Miller, R. D.; Michl, J. *Chem. Rev.* **1989**, *89*, 1359.
(10) Furukawa, S.; Takeuchi, K.; Shimana, M. *J. Phys.: Condens. Matter* **1994**, *6*, 11007.
(11) Yamakawa, H.; Fujii, M. *Macromolecules* **1974**, *7*, 128.
(12) Yamakawa, H.; Yoshizaki, T. *Macromolecules* **1980**, *13*, 633.
(13) Benoit, H.; Doty, P. M. *J. Phys. Chem.* **1953**, *57*, 958.
(14) Sato, T.; Terao, K.; Teramoto, A.; Fujiki, M. *Macromolecules*, submitted.
(15) Cotts, P. M.; Miller, R. D.; Trefonas III, P. T.; West, R.; Fickes, G. N. *Macromolecules* **1987**, *20*, 1046.
(16) From the reaction process, the terminal group of our PD2MBS samples is expected to be a hydrogen atom.
(17) Terao, K.; Hokajo, T.; Nakamura, Y.; Norisuye, T. *Macromolecules* **1999**, *32*, 3690.
(18) Sato, T.; Jinbo, Y.; Teramoto, A. *Macromolecules* **1997**, *30*, 590.
(19) Yoshizaki, T.; Nitta, I.; Yamakawa, H. *Macromolecules* **1988**, *21*, 165.
(20) Khokhlov, A. R.; Semenov, A. N. *Physica A* **1981**, *108A*, 546.
(21) Onsager, L. *Ann. N. Y. Acad. Sci.* **1949**, *51*, 627.
(22) DuPré, D. B.; Yang, S. *J. Chem. Phys.* **1991**, *94*, 7466.
(23) Maeno, K.; Nakamura, Y.; Terao, K.; Sato, T.; Norisuye, T. *Kobunshi Ronbunshu* **1999**, *56*, 254.

MA0110352